COLORADO STATE
UNIVERSITY
FORT COLLINS, COLORADO
80521

department
of
electrical
engineering

ENTRAINMENT IN ELECTROHYDRODYNAMIC HEAT PIPES

NASA CR-114499

AVAILABLE TO THE PUBLIC

Research Report #2

August, 1972

by T. B. Jones and M. P. Perry

NASA Grant # NGR-06-002-127

prepared for
Ames Research Center
National Aeronautics and Space Administration
Moffett Field, California 94035

ENTRAINMENT IN ELECTROHYDRODYNAMIC HEAT PIPES

NASA CR-114499

Research Report #2

August, 1972

by T. B. Jones and M. P. Perry

Department of Electrical Engineering

Colorado State University

Ft. Collins, Colorado 80521

NASA Grant # NGR-06-002-127

prepared for

Ames Research Center

National Aeronautics and Space Administration

Moffett Field, California 94035

TABLE OF CONTENTS

LIST OF FIGURES

I. Introduction

Entrainment is one of the limits imposed upon the operation of capillary heat pipes.[1] It occurs when the vapor counterflow is fast enough to shear off tiny drops of liquid from exposed liquid surface areas in the capillary structure. These drops are swept along or entrained with the vapor flow. The noisy impingement of these droplets at the condenser end of a heat pipe has been cited as the primary evidence of this phenomenon.[2]

A modification of the so-called Kelvin-Helmholtz interfacial instability[3] plays a primary role in establishing the conditions for this phenomenon. The criterion for avoidance of this instability is often used by designers as a conservative estimate of the likelihood of the occurrence of entrainment in their heat pipes. If

$$We \equiv \frac{\rho_v V_v^2/2}{\gamma/r_o} < 1 \quad , \tag{1}$$

where ρ_v = vapor density,

V_v = vapor velocity,

γ = surface tension,

r_o = capillary pore size,

entrainment is assumed to be of no importance. One may easily deduce this criterion from Lamb's work[3] by making the recognition that the wick structure restricts unstable wavelengths to values less than the effective capillary pore size. The more common derivation of Eq. (1) is based upon the comparison of vapor dynamic pressure and liquid surface tension forces.

This familiar background is of interest in connection with the electrohydrodynamic heat pipe because this new device with its extensive free surface area is apt to exhibit a modified type of entrainment. The liquid-vapor interface is maintained in equilibrium by the electric field polarization force; this force thus becomes important in counteracting the vapor shear. A simple dimensional analysis might suggest the following as a criterion for the avoidance of this instability.[4]

$$We^{E} \simeq \frac{\rho_v V_v^2}{(\epsilon_\ell - \epsilon_v) E_o^2} < 1 \quad , \tag{2}$$

where E_o is the tangential electric field intensity measured at the interface, and ϵ_ℓ and ϵ_v are the liquid and vapor dielectric constants, respectively. This simple result is, however, not complete, as analysis of a relevant electric field coupled interfacial stability problem shows.

II. Theory

A. The Model

Following methods similar to those of Melcher,[5] the general problem posed in the Figure 1 is considered. The dielectric liquid (below) moves with a uniform velocity profile in the $+\hat{x}$ direction; the vapor (above) moves in the opposite direction, also with a uniform velocity profile. This inviscid model, originally attributed to Rayleigh,[6] results in a non-allowable flow discontinuity between the liquid and vapor flows; large shear forces are present at this interface which in general are not negligible. Based upon this argument significant objection may be raised concerning the validity of the model.[7] Still, for the purpose of deriving a general design criterion similar to Eq. (1), the inadequacies of the model are overlooked here.

The interface is assumed to reside in the region of an electric field, mutually perpendicular to the $\hat{x}$ and $\hat{y}$ directions. This field is E_o at the interface ($y = 0$), but exhibits a mild gradient, decreasing in the $+\hat{n}$ direction. Note that purely x-dependent surface perturbations ξ, of the assumed form

$$\xi(x,t) = \mathrm{Re}\,[\hat{\xi}e^{j(\omega t - kx)}] \quad , \quad |\hat{\xi}| << 2\pi/k \tag{3}$$

do not significantly disturb the electric field. The surface is in equilibrium at $y = 0$.

B. EHD-Coupled Kelvin-Helmholtz Instability

The fluid equations for both the liquid and vapor are of similar form.

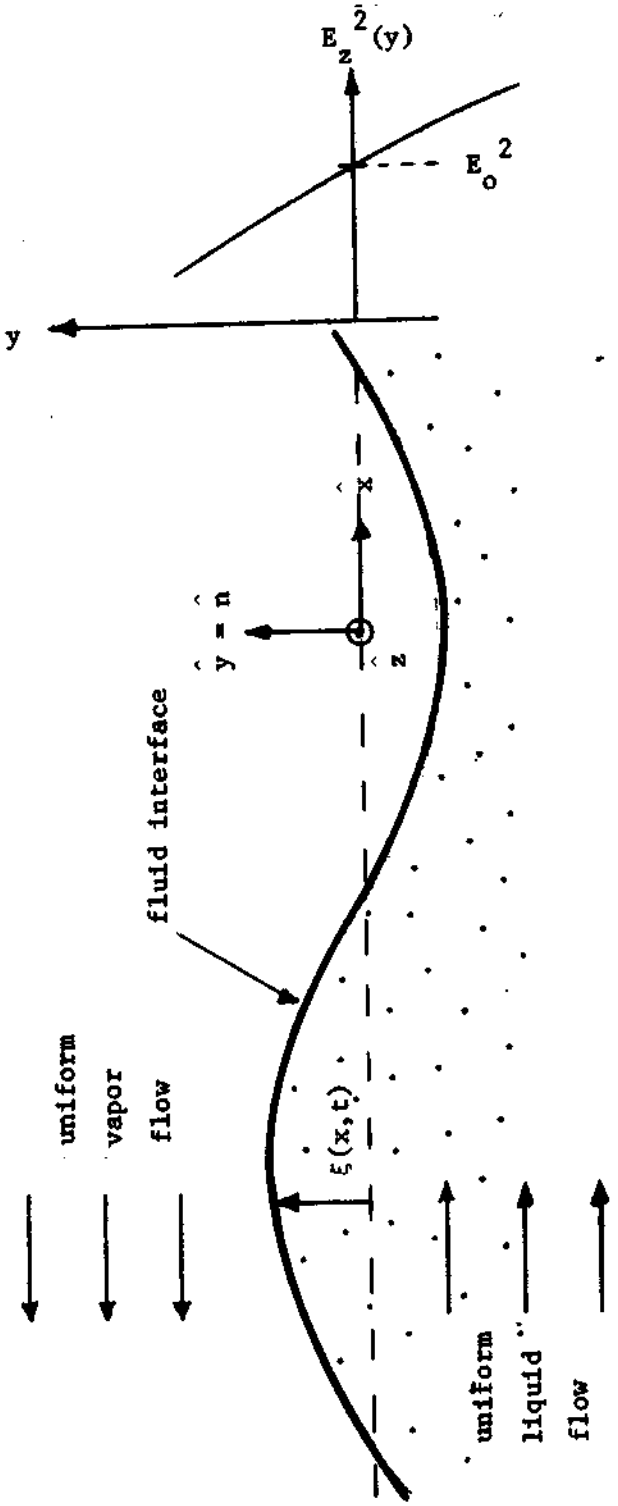

Figure 1. Dielectric liquid interface with nonuniform tangential electric field perpendicular to vapor shear flow.

$$\rho_i\left(\frac{\partial}{\partial t} + V_i \frac{\partial}{\partial x}\right) v_i = - \nabla p_i - \rho_i g \hat{y} \tag{4}$$

$$\nabla \cdot \bar{v}_i = 0 \tag{5}$$

The incompressibility assumption for the vapor is valid, due to the low vapor velocities considered. Combination of Eq.'s (4) and (5) yields

$$\nabla^2 p_i' = 0 \tag{6}$$

for the liquid or vapor perturbation pressure. Consistent with Eq. (3), assume

$$p_i'(x,y,t) = \text{Re}\ [\hat{p}_i(y) e^{j(\omega t - kx)}] \tag{7}$$

as typical of the spatial dependence of all perturbation mechanical variables. Use of the boundary conditions

$$\text{liquid:} \quad v_y(x, y = \xi_-, t) = \text{Re}\ [j(\omega - kV_\ell)\hat{\xi} e^{j(\omega t - kx)}] \tag{8}$$

$$\text{vapor:} \quad v_y(x, y = \xi_+, t) = \text{Re}\ [j(\omega + kV_v)\hat{\xi} e^{j(\omega t - kx)}] \tag{9}$$

yields the result for the perturbation pressure quantities measured at the interface.

$$\hat{p}_\ell(y = \xi, t) = \frac{\rho_\ell(\omega - kV_\ell)^2}{k} \hat{\xi} - \rho_\ell g \hat{\xi} \tag{10}$$

$$\hat{p}_v(y = \xi, t) = -\frac{\rho_v(\omega + kV_v)^2}{k} \hat{\xi} - \rho_v g \hat{\xi} \tag{11}$$

The surface equation balances the pressure forces against surface tension and the electric polarization force.

$$\hat{p}_\ell - \hat{p}_v = k^2\gamma\hat{\xi} - \delta\hat{T}^e(\hat{\xi}) \tag{12}$$

where $\delta\hat{T}^e(\hat{\xi})$ is the perturbation electric stress

$$\delta\hat{T}^e = \delta\left[\frac{(\varepsilon_\ell-\varepsilon_v)E_o^2}{2}\right], \quad (E_o > 0) \quad , \tag{13}$$

$$= -(\varepsilon_\ell-\varepsilon_v)E_o\left|\frac{\partial E}{\partial\xi}\right|_o\hat{\xi} \quad , \tag{14}$$

and the quantity $\frac{\partial E}{\partial\xi}_o$ is always negative for our case.

The dispersion relation relates the eigenvalues ω and k. It is obtained by substituting Eq. (14) into Eq. (12) and canceling out $\hat{\xi}$. Expressed as a polynomial in ω, it is

$$\omega^2 + b(k)\omega + c(k) = 0, \tag{15}$$

where

$$b(k) = -2k\left[\frac{\rho_\ell V_\ell - \rho_v V_v}{\rho_\ell + \rho_v}\right], \tag{16}$$

and

$$c(k) = \frac{k^2(\rho_\ell V_\ell^2 + \rho_v V_v^2)}{\rho_\ell + \rho_v} - \left(\frac{\rho_\ell - \rho_v}{\rho_\ell + \rho_v}\right) gk$$

$$- \frac{k^3\gamma}{\rho_\ell + \rho_v} - k\left(\frac{\varepsilon_\ell - \varepsilon_v}{\rho_\ell + \rho_v}\right) E_o \left|\frac{\partial E}{\partial\xi}\right|_o . \tag{17}$$

Absolute instability occurs if, for some real value or values of k, the frequency ω exhibits a negative imaginary component. For this case, the initially small displacement $\xi(x,t)$ grows exponentially in time, until

some nonlinear mechanism alters or inhibits further growth. Thus, this absolute instability criterion does not necessarily predict the onset of entrainment, but only the initial amplification of small perturbations from which entrainment may result. Such a criterion may be safely used as a conservative design factor.

C. The Stability Criterion

It is helpful to define a new dimensionless quantity,

$$We' = \frac{\left(\frac{\rho_\ell \rho_v}{\rho_\ell + \rho_v}\right) V^2}{\left\{4\gamma \left[(\rho_\ell - \rho_v)g + (\varepsilon_\ell - \varepsilon_v)E_o \left|\frac{\partial E}{\partial \xi}\right|_o\right]\right\}^{1/2}} \tag{18}$$

where $V \equiv V_v + V_\ell$.

The magnitude of We' is easily shown to determine stability .

(i) We' < 1, stable.

(ii) We' = 1, marginal stability of single wavenumber,

$$k^* = \frac{\rho_\ell \rho_v V^2}{2\gamma(\rho_\ell + \rho_v)} \quad . \tag{19}$$

(iii) We' > 1, unstable band of wavenumbers.

D. Discussion

The surface tension continues to play a role in the entrainment limit of electrohydrodynamic heat pipes, as evidenced by Eqs. (18) and (19), and the stability criterion itself. This conclusion is not surprising, because of the nature of the instability itself. As opposed to the nature of a capillary wick, the surface of the liquid in an EHD flow structure is open, with no restrictions placed upon the wavenumbers of likely perturbations. Thus, the wavenumber with the maximum temporal growth rate

plays the crucial role in instability. Both surface tension, which strongly stabilizes the larger wavenumbers, and the electric field, which strongly stabilizes the smaller wavenumbers, must be used to calculate k^*.

If it is found experimentally that entrainment in EHD heat pipes presents an unusually severe operating constraint, the means exist to alleviate the problem. See Fig. 2. Here the free surfaces along at least part of the length of the EHD flow structure of a heat pipe are baffled with some insulating wick material (e.g., Refrasil).

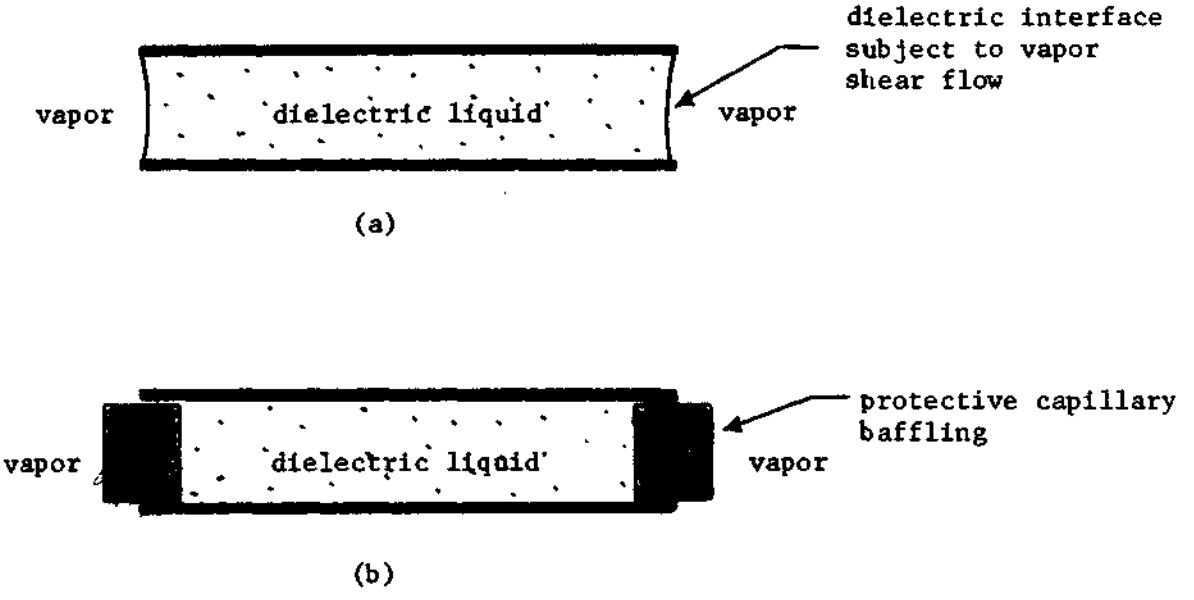

Figure 2. Parallel-plate EHD flow structures: (a) with dielectric interface subject to vapor shear and possible Kelvin-Helmholtz instability; (b) with capillary baffling.

III. Experiment

A. Experimental Geometry

The experimental apparatus shown in Figure 3a and b was used to test the simple theory described above. A rectangular channel 6" long, 1" wide and 1/2" deep was equipped with an array of 1/16" diameter brass rods which served as electrodes. These rods were flush with the top of the channel and were connected with alternate polarity to a high voltage a-c power supply (400 Hz). With the liquid surface flush with the tops of the electrode rods, an essentially tangential electric field with a negative gradient away from the liquid could be imposed.

The entire channel structure shown in Figure 3 was placed inside a long plexiglas enclosure with a variable speed fan at one end. The speed of the air flow was controlled by adjusting a rheostat, and it was measured with a pitot tube and an inclined manometer. The accuracy of air speed measurements was estimated at 10%.

Care was taken to keep the liquid surface flush with the bottom of the wind tunnel. This step minimized the incidence of turbulent eddies and made the onset of the Kelvin-Helmholtz instability a more distinct and observable transition. See Figure 4.

B. Procedure

After filling the channel so that the liquid surface just covered the electrode rods (see Fig. 3b), the voltage was turned up to a relatively high value. Then the fan was turned on to a predetermined speed. With the voltage high enough, the liquid surface remained quiescent, stabilized by the electric field gradient force. The voltage was slowly turned down until small amplitude

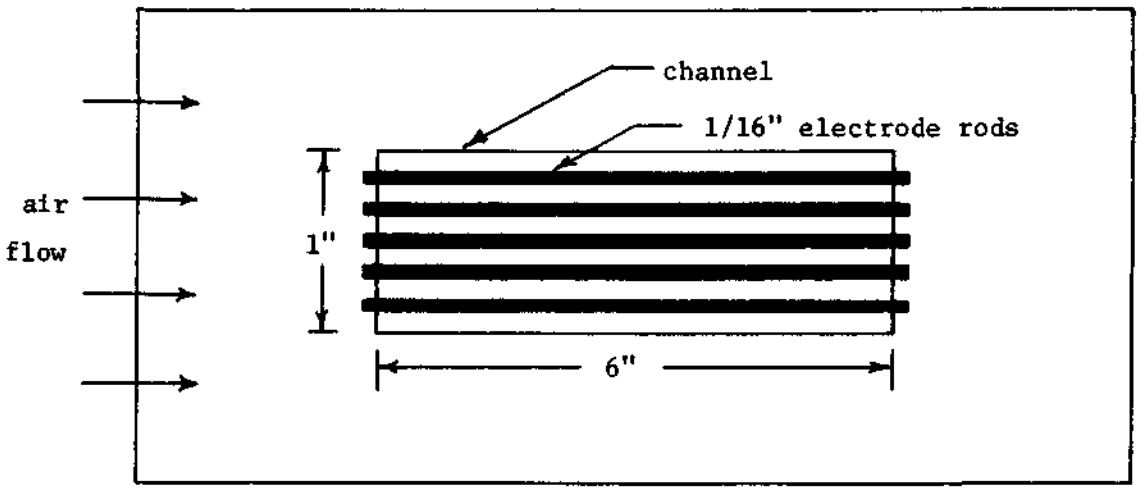

(a) Top view of fluid channel apparatus.
(Not drawn to scale).

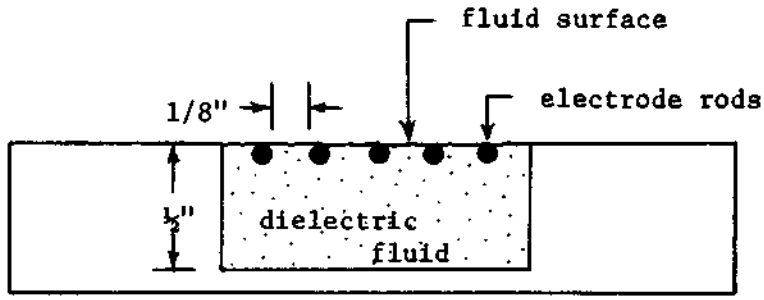

(b) Cross-sectional view of fluid channel.
Note that fluid fills reservoir level with the top of the channel and with the electrode rods.

Figure 3. Experimental fluid channel used to study EHD-coupled Kelvin-Helmholtz instability.

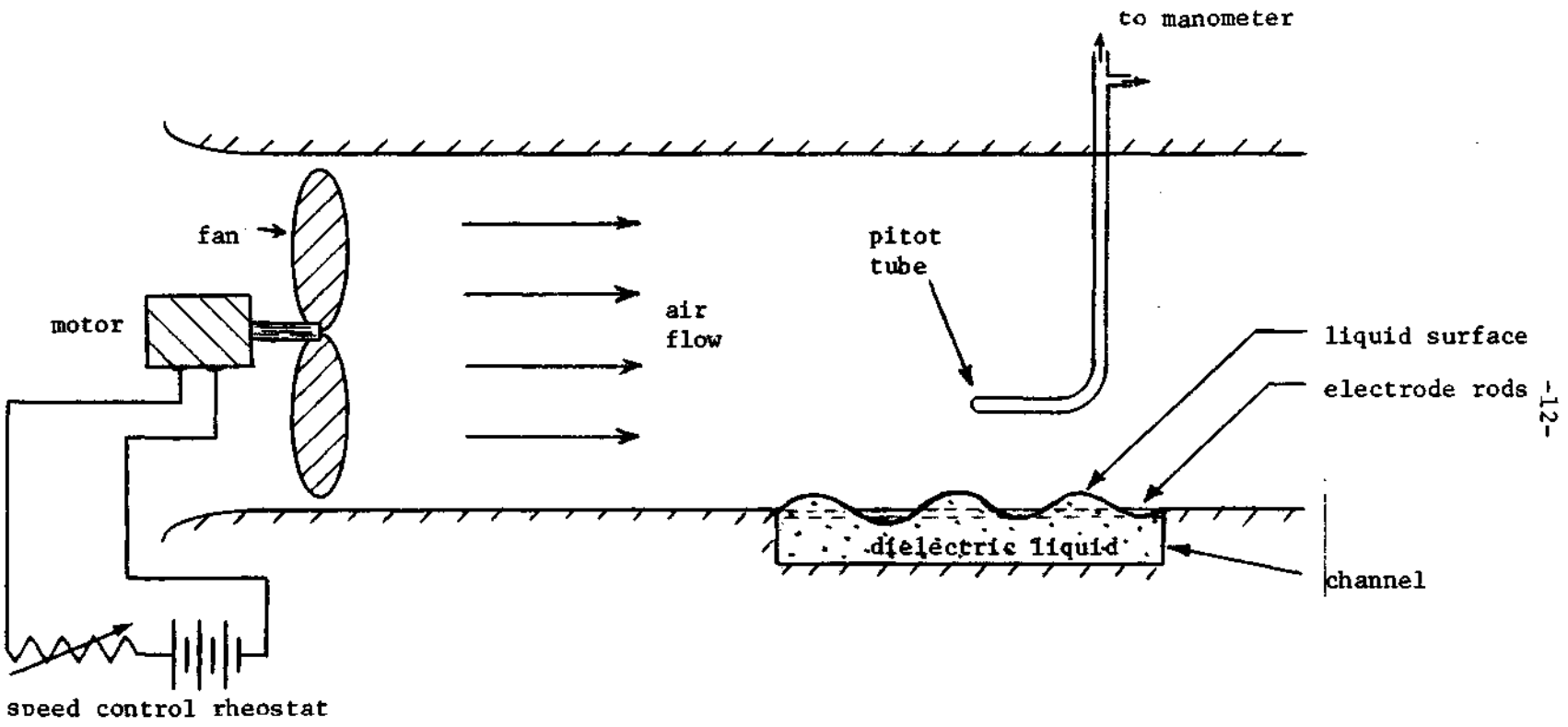

Figure 4. Wind tunnel used in experiments, showing fluid channel placement.

wave-like disturbances were seen to develop. This value of voltage, measured by an electrostatic voltmeter, was taken as the marginal stability point for the given air speed. The voltage was quite distinct and reproducible; further decrease of the voltage always produced large nonlinear disturbances which washed downstream and spilled out of the channel. Increasing the voltage once again always stabilized the surface.

C. Results

The data are plotted in Figures 5a and b, which show the relation between voltage and air speed at the transition between stable and unstable regimes. The theoretical curves shown result from setting We' of Eq. (18) to unity. Values above the curve are unstable and values below are stable. Note the rather good agreement of the experimental data with the theoretical curve for both corn oil and transformer oil.* (The properties of these liquids are given in Appendix A.) The small difference between the theory and experiment can be accounted for partially by measurement uncertainties, but also by the limitations of the theoretical model chosen for the Kelvin-Helmholtz instability. Further, the value of $\left|\frac{\partial E}{\partial \xi}\right|_o$ chosen for the theoretical calculation is somewhat suspect, due to transverse variation of this quantity at the liquid surface.

- - - - - - - - - -

* Due to the tendency of Freon-113 to evaporate rapidly when the air flow was introduced, no data for this important dielectric fluid was obtained.

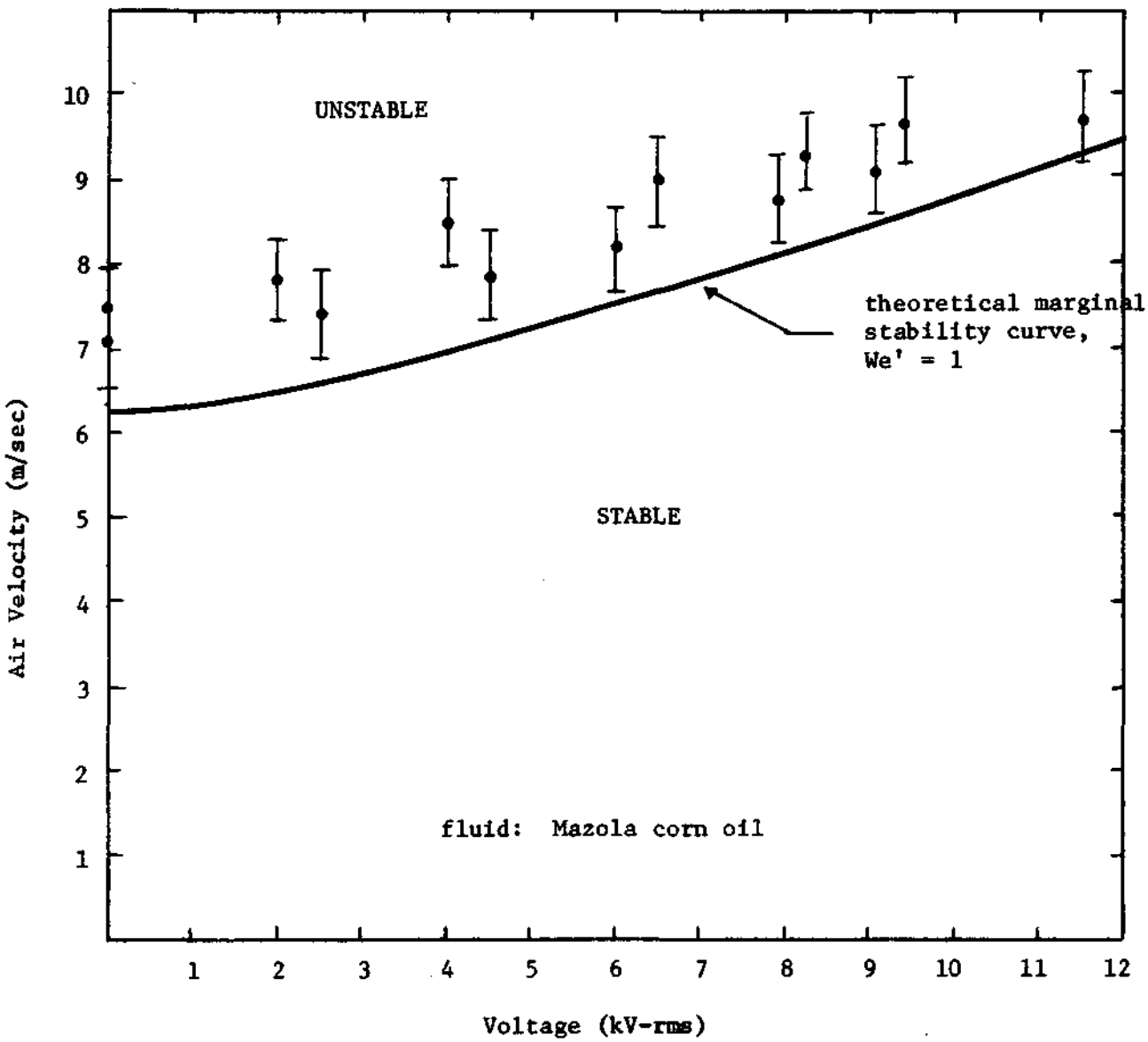

Figure 5. (a) Experimental marginal stability data with theoretical plot. Fluid is Mazola corn oil.

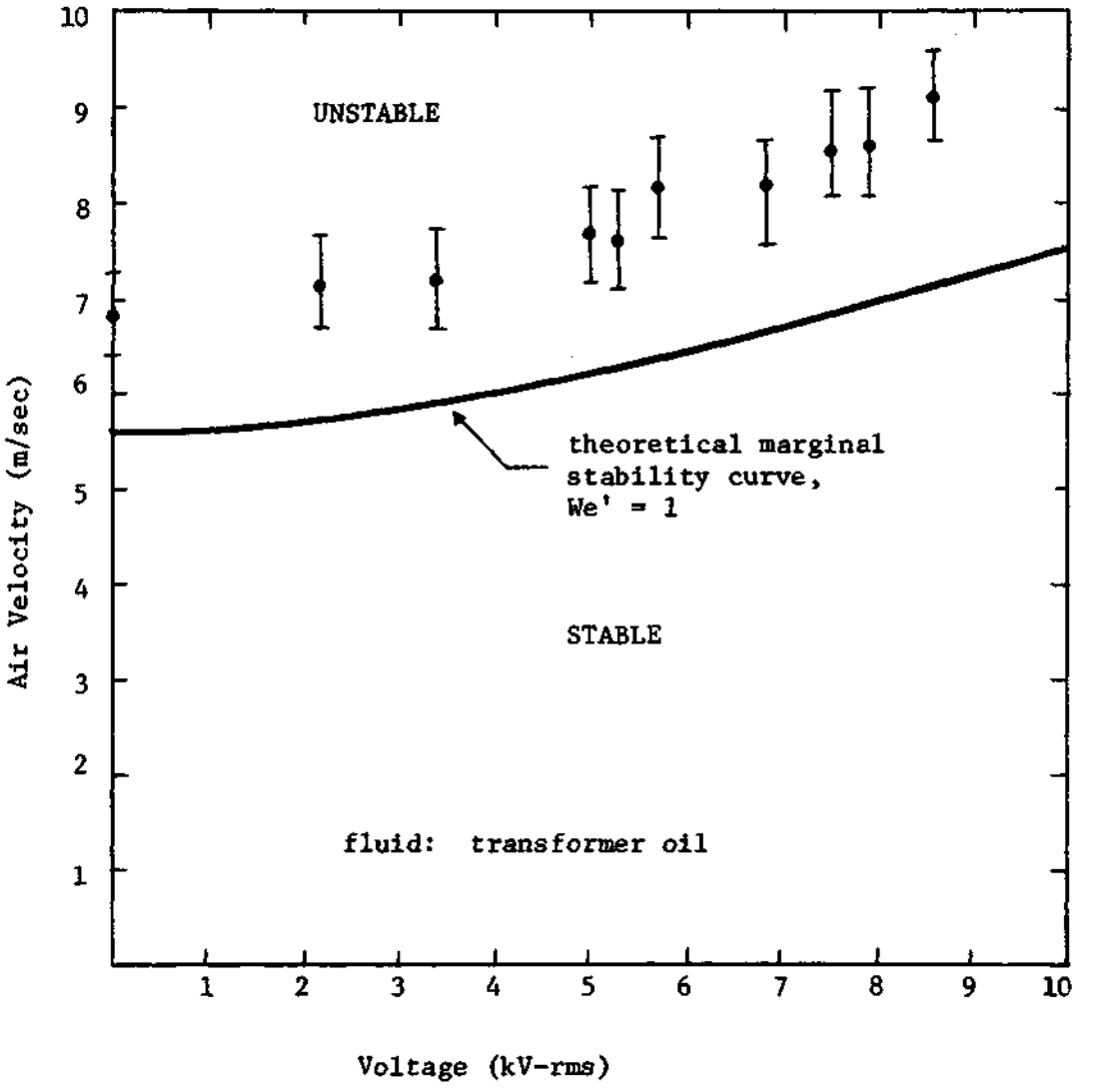

Figure 5. (b) Experimental marginal stability data with theoretical plot. Fluid is G.E. 10-C transformer oil.

IV. Conclusion

The success of the theoretical analysis in predicting onset of the Kelvin-Helmholtz instability is the best justification of the work reported here. Still, the lack of data on freon or other much less viscous dielectric liquids, and the relative simplicity of the electrode structure used in these experiments introduce some uncertainty as to the general applicability of the criterion developed and tested here to typical EHD heat pipes. The difficulty of performing well-controlled laboratory experiments with the flow structures typical of an EHD heat pipe preclude a more complete test of the theory at this time.

APPENDIX A

PROPERTIES OF SOME DIELECTRIC FLUIDS

(@ 72° F)

fluid	density (kg/m^3)	dynamic viscosity $\left(\frac{kg - m^2}{sec}\right)$	relative dielectric constant	surface tension (N/m)
Mazola Corn Oil	$0.91 \cdot 10^3$	$5.46 \cdot 10^{-2}$	3.1	0.062
G.E. 10-C transformer oil	$0.87 \cdot 10^3$	$\sim 10^{-2}$	2.56	0.04
Dupont Freon-113	$1.57 \cdot 10^3$	$0.68 \cdot 10^{-3}$	2.41	0.019

APPENDIX B

Nomenclature

$\overline{E}$	=	electric field vector
E_o	=	tangential electric field at fluid surface
g	=	gravitational acceleration (9.81 m/sec^2)
j	=	$\sqrt{-1}$
k	=	wavenumber
$\hat{n}$	=	unit vector normal to fluid surface
p	=	fluid pressure
r_o	=	effective capillary pore size
t	=	time
V	=	fluid velocity
We	=	capillary Weber number
We^E, We'	=	electric Weber numbers
x, y, z	=	coordinate axes
γ	=	surface tension
ϵ	=	dielectric constant
ρ	=	fluid density
ω	=	radian frequency
ξ	=	fluid surface displacement

Subscripts:

ℓ -- liquid

v -- vapor

REFERENCES

1. Kemme, J. E., "Heat Pipe Design Considerations," Los Alamos Scientific Laboratory, Report #LA-4221-MS, August, 1969.

2. Kemme, J. E., and Florschuetz, L. M., "Sonic Limitations and Startup Problems of Heat Pipes," Los Alamos Scientific Laboratory, Report #LA-4518, September, 1970.

3. Lamb, H., Hydrodynamics, art. 268, Dover, New York, 1945.

4. Jones, T. B., "The Feasibility of Electrohydrodynamic Heat Pipes," Research Report #1, NASA CR-114392, Department of Electrical Engineering, Colorado State University, Ft. Collins, Colorado, October, 1971.

5. Melcher, J. R., Field-Coupled Surface Waves, Chapter 3, MIT Press, Cambridge, Mass., 1963.

6. Lord Rayleigh, The Theory of Sound, vol. 2, art. 365, Dover, New York, 1945.

7. Lin, C. C., Theory of Hydrodynamic Stability, Chapter 4, Cambridge University Press, London, 1955.